# Effects of lattice anisotropy and temperature on domain growth in the two-dimensional Potts model

Elizabeth A. Holm
*Department of Materials Science and Engineering, The University of Michigan, Ann Arbor, Michigan 48109-2136*

James A. Glazier*
*AT&T Bell Laboratories, Murray Hill, New Jersey 07974-2070*

David J. Srolovitz
*Department of Materials Science and Engineering, The University of Michigan, Ann Arbor, Michigan 48109-2136*

Gary S. Grest
*Corporate Research Science Laboratory, Exxon Research and Engineering Company, Annandale, New Jersey 08801*
(Received 4 October 1990)

Two-dimensional, infinitely degenerate Potts-model simulations were performed on four different lattices at zero and finite temperatures in order to examine the effects of lattice anisotropy and temperature on domain growth. The discrete lattice of the Potts model causes deviations from universal domain growth behavior by weakening the vertex angle boundary conditions that form the basis of von Neumann's law. Smoothing the Wulff plot of the lattice (e.g., by extending spin interactions to a longer range) or increasing the temperature at which the simulation is performed can overcome the anisotropy inherent in discrete lattice simulations. Excellent overall agreement (kinetics, topological distribution, domain size distributions) between the low lattice anisotropy Potts-model simulations and the soap froth suggests that the Potts model is useful for studying domain growth in a wide variety of physical systems.

## I. INTRODUCTION

Many quasi-two-dimensional materials exhibit threefold connected, cellular patterns which coarsen in time as some domains grow and others shrink and disappear.[1-3] The dynamics for curvature driven diffusive coarsening, assuming 120° vertex angles and minimal surface domain boundaries, follow a quantitative relation between the number of sides and rate of domain growth, known as von Neumann's law,[4]

$$\frac{da_n}{dt}=\kappa(n-6) \tag{1}$$

where $a_n$ is the area of an $n$-sided domain and $\kappa$ a diffusion constant. Domain growth in the low-temperature, infinitely degenerate Potts model proceeds by a discrete form of curvature driven domain wall migration. Empirically, the two-dimensional soap froth and the Potts model both obey von Neumann's law.

When domains disappear, their remaining neighbors gain or lose sides. The manner in which this side redistribution occurs determines the topological evolution of the pattern. In particular, arbitrary initial patterns evolve into scaling states in which the topological distribution functions [$P(n)$, the probability that a domain has $n$ sides] and the area distribution functions [$P(a/\langle a\rangle)$, the probability that a domain has a given fractional area $a$ with respect to the mean domain area $\langle a\rangle$] remain constant, while the length scale increases with time. These distribution functions depend only on the underlying dynamics and the nature of side redistribution. In an idealized model, all domains would grow according to von Neumann's law and all walls would take the form of minimal surfaces. Side redistribution would result deterministically from this minimal surface constraint. Weaire and Kermode,[5] Frost and Thompson,[6] Kawasaki, Nagai, and Nakashima,[7] and Soares, Ferro, and Forres[8] have studied a variety of explicit approximations to this ideal.

Qualitatively, the Potts model evolves an initial pattern into a scaling state in a manner similar to that observed in real soap froths and metal foils.[1] This resemblance implies that side redistribution is comparable in the three cases. However, quantitative comparisons between the scaling state distribution functions reveal significant differences, with the Potts-model results intermediate between those of the metal and the soap froth. Since the Potts model has become the *de facto* standard model for domain growth, it is imperative to delineate the differences and similarities between the Potts model and experimental domain growth.

The Potts model (and the foil) differ in two fundamental ways from the soap froth.[9] In the soap froth, the diffusion of gas across cell walls, which is much slower than the readjustment of the soap films subject to stress, drives coarsening of the pattern. Thus the walls of a soap froth approximate minimal surfaces. In the Potts model and in metallic grain growth, the basic growth process is diffusion of atoms across grain boundaries. Since the rate of diffusion across the boundary (causing grain growth) and the rate of diffusion along it (causing changes in boundary shape) are comparable, grain boundaries take shapes that can be far from ideal minimal surfaces. The

 

second difference is that the surface tension of soap froth is entirely isotropic, whereas the energy per unit length of a grain boundary in a Potts model or metal depends on its orientation with respect to a crystal lattice. Just as thermal fluctuations and entropy effectively decrease the anisotropy of a Wulff (surface energy versus surface orientation) plot at elevated temperatures, we expect that lattice anisotropy effects should decrease with increasing temperature. Hence the evolution of the Potts model and metals should become more similar to soap froth at higher temperatures. Note, however, that the lattice orientation of a metal varies from grain to grain while the lattice in the Potts model is homogeneous.

While lattice anisotropy is unquestionably present in the Potts model, the main features of domain growth (e.g., the temporal scaling of domain size) are unaffected by small changes in anisotropy. In fact, the overall agreement between the evolution of a soap froth and a Potts model starting from similar conditions is very good. However, $T=0$ Potts-model simulations carried out by Glazier, Anderson, and Grest[1,9] show a consistently slower transition from order to disorder than the froth. Even in the scaling state, the Potts model consistently yields wider side and area distributions than the soap froth. In addition, Potts-model domain boundaries tend to lie preferentially along low-energy crystalline axes. In this paper we examine in detail the effects of lattice anisotropy and temperature on Potts-model coarsening to try to understand the origin of these discrepancies.

## II. THE POTTS MODEL

Potts-model simulations of domain growth have been discussed in other publications.[10–16] The Potts Hamiltonian is

$$H=J\sum_{(i,j),(i',j')}1-\delta_{\sigma_{(i,j)}\sigma_{(i',j')}} \tag{2}$$

where $J$ is a positive constant, $\delta$ is the Kronecker delta function, $1\leq\sigma_{(i,j)}\leq N_d$ denotes the orientation of the spin at site $(i,j)$, $N_d$ is the number of domains in the system at the beginning of the simulation, and $(i,j),(i',j')$ represents $(i,j),(i',j')$ neighbors. Evolution proceeds by a Monte Carlo procedure in which a spin is selected at random and converted to a new random orientation with probability $p=e^{-\Delta E/kT}$ where $\Delta E$ is the change in system energy produced by the reorientation. After each reorientation attempt, time is incremented by $1/N_\sigma$ Monte Carlo steps (MCS), where $N_\sigma$ is the number of lattice spin sites in the system. At $T>T_c$ the system is disordered, while at $T<T_c$ a well-defined domain structure evolves. At $T=0$, these domains are simply connected; however, at finite temperatures small domains may nucleate within a larger domain. In order to alleviate the effects of these fluctuations, we quench each finite temperature simulation to $T=0$ for a short time prior to enumerating the domain size and side distributions. Since the average number of sides per domain $\langle n\rangle=6$ for simply connected domains, the duration of the quench is adjusted such that $5.98<\langle n\rangle<6.02$. Similarly, to prevent domain coalescence, domains are numbered so that no two domains have identical spins, resulting in an infinitely degenerate system.

We study the anisotropy of the Potts model by performing identical simulations on a variety of lattices with different anisotropies and at a variety of temperatures. We characterize the anisotropy by the ratio of the highest- to the lowest-energy domain boundary orientations. The highest possible anisotropy occurs for the nearest-neighbor honeycomb lattice. However, steady state domain growth does not occur on this lattice at any temperature. We therefore confine our study to the nearest- and next-nearest-neighbor square lattices [$s(1)$ and $s(1,2)$, respectively] and the nearest- and next-nearest-neighbor triangular lattices [$t(1)$ and $t(1,2)$, respectively] at $T=0$, $T=\frac{1}{3}T_c$, and $T=\frac{2}{3}T_c$.[17,18] The lattice anisotropies $\eta$ for these lattices are $\eta_{s(1)}=1.414$, $\eta_{s(1,2)}=1.116$, $\eta_{t(1)}=1.154$, and $\eta_{t(1,2)}=1.057$.[19] All runs employ $200\times200$ lattices with periodic boundary conditions. All simulations were performed by quenching from $T\gg T_c$ to $T<T_c$ at 0 MCS, and we average ten independent simulations to produce each complete run.

## III. KINETICS

The basic measure of the evolution of domain structure is the average domain size as a function of time. Any system obeying von Neumann's law reaches a scaling state in which

$$\langle a(t)\rangle^{1/\alpha}-\langle a(0)\rangle^{1/\alpha}=\gamma t\ , \tag{3a}$$

$$\langle a(t)\rangle\propto t^{\alpha} \tag{3b}$$

where Eq. (3b) is valid for $\langle a(t)\rangle\gg\langle a(0)\rangle$, $\gamma$ is a positive constant, and $\alpha=1$. Deviations from $\alpha=1$ are common experimentally and indicate the presence of additional effects besides ideal von Neumann's law coarsening; for example, finite fluid fraction in soap froths[20,21] and impurities in metals[2,22] result in lower growth rates at long times and hence lower exponents. Generally, the domain growth exponent $\alpha$ gradually increases as the system approaches steady state.[23]

Figure 1 shows the temporal evolution of the mean domain area $\langle a\rangle$. In the $t(1,2)$, $s(1,2)$, and $t(1)$ lattices at all temperatures, the rate of growth of $\langle a\rangle$ increases monotonically in time to a value consistent with the large-system asymptotic exponent $\alpha=1$.[13] For the $s(1)$ lattice, theory predicts that zero temperature domain growth halts when the domain vertices absorb all intial wall curvature; however, domain wall fluctuations which occur at any finite temperature enable domain growth to proceed to completion.[11,24,25] Figure 1 shows that domain growth stops at approximately $10^3$ MCS in the $s(1)$ system at $T=0$ and does not recommence during the $10^6$ MCS of the simulation. In contrast, the rate of domain growth in the $s(1)$ lattice at $\frac{2}{3}T_c$ increases monotonically to a rate consistent with $\alpha=1$ in a manner similar to the $t(1,2)$, $s(1,2)$, and $t(1)$ lattices. The $T=\frac{1}{3}T_c$ $s(1)$ lattice is an interesting intermediate case. Domain growth halts for a long interval but eventually resumes and reaches a scaling state consistent with $\alpha=1$.

Presumably, this stagnant period is the time required for thermal nucleation of a sufficient density of kinks on the domain walls to balance the kink or curvature absorption at vertices.

The presence of the finite initial domain size term $\langle a(0)\rangle$ in Eq. (3a) guarantees that the slope of the $\log_{10}\langle a\rangle$ versus $\log_{10}t$ plots must increase to $\alpha$ at long times. While the simulations on all of the lattices have the same intial domain size, the prescaling region in Fig. 1(a) depends on both lattice anisotropy and temperature,

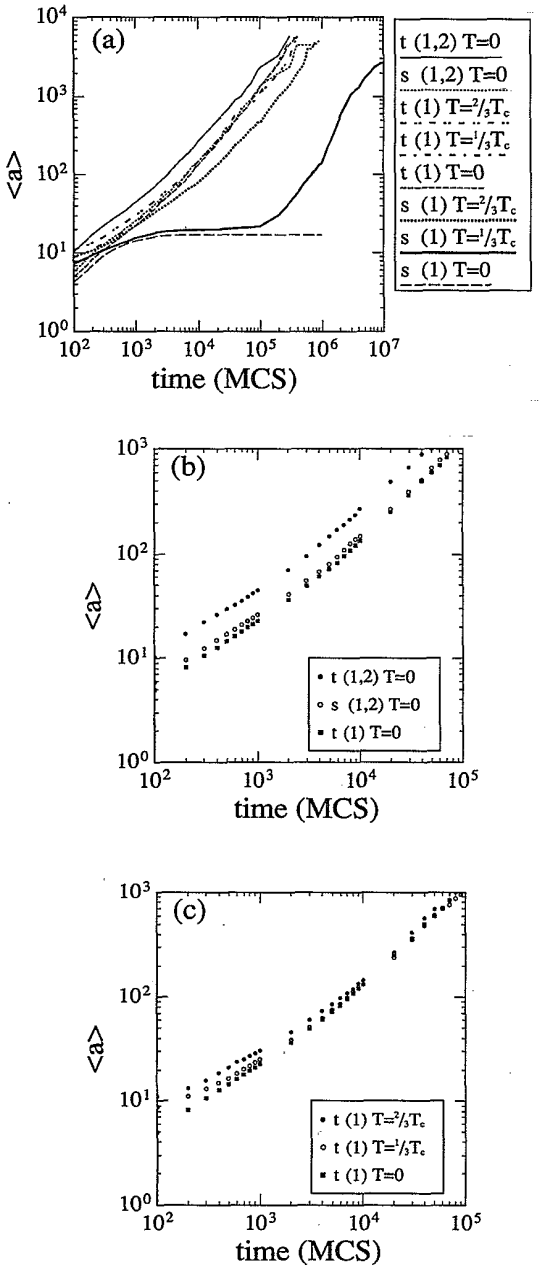


FIG. 1. Kinetics of Potts-model domain growth. (a) Mean domain area vs time for $s(1)$ and $t(1)$ at $T=0$, $\frac{1}{3}T_c$, and $\frac{2}{3}T_c$, and $s(1,2)$ and $t(1,2)$ at $T=0$. (b) Effect of lattice anisotropy on early time domain growth at $T=0$. (c) Effect of temperature on early time domain growth in the $t(1)$ lattice,

so there is clearly an effect of the discrete lattice for which the continuum growth law represented by Eq. (3) does not account.

We show the effect of lattice anisotropy on domain growth in Fig. 1(b). Assuming that the anisotropy is not too large for domain growth to occur [see $s(1)$ at $T=0$ in Fig. 1(a)], increases in lattice anisotropy decrease the growth rate at early time ($t<10^2$ MCS). Following this very early growth rate dependence on lattice anisotropy, the domain coarsening rate becomes independent of anisotropy; hence, all of the curves in Fig. 1(b) are parallel at later times ($t>10^2$ MCS).

We show the effect of temperature on domain growth in Fig. 1(c) where we plot the domain growth kinetics for the $t(1)$ lattice at $T=0$, $\frac{1}{3}T_c$, and $\frac{2}{3}T_c$. At the earliest times ($t<10^2$ MCS), the domains of the highest-temperature system grow the fastest. Then, at intermediate times, the growth kinetics cross over (around $t=2\times10^4$ MCS) to temperature-independent behavior.

Since all of the simulations tend to the same scaling behavior at long times or large domain sizes, the discreteness of the lattice is unimportant to domain growth kinetics in the long-time regime. In contrast, at early times, decreasing lattice anisotropy or increasing temperature tend to reduce the kinetic effects of lattice discreteness and increase growth rates. Likewise, the discreteness of the atomic lattice in grain growth, in effect, decreases with increasing temperature, as evinced in the experimentally observed increase in grain growth exponents with increasing temperature.[26] However, as Figs. 1(b) and 1(c) demonstrate, temperature and lattice anisotropy are not equivalent variables.

## IV. EFFECTS OF LATTICE ANISOTROPY ON DISTRIBUTIONS

Scaling state domain edge and domain area distributions are shown in Figs. 2(a) and 2(b), respectively. The curves display significant noise due to the small number of domains present in the scaling state (approximately 350); however, the curves for the systems which grow normally [$t(1,2)$, $s(1,2)$, and $t(1)$ at all temperatures and $s(1)$ at $T=\frac{2}{3}T_c$] appear very similar in shape. In contrast, edge and area distributions for the systems which experience some degree of lattice pinning [$s(1)$ at $T=0$ and $\frac{1}{3}T_c$] are fundamentally different from the rest. Since the stable pinned domain on the square lattice is a square, the edge distributions for $s(1)$ at $T=0$ and $\frac{1}{3}T_c$ show no domains with $n<4$. Likewise, the area distribution for the $T=0$ square lattice is truncated at an area close to the mean area. The area distribution of the scaling state $T=\frac{1}{3}T_c$ square lattice is intermediate between the pinned $T=0$ case and the normally growing $T=\frac{2}{3}T_c$ case. Thus the domain edge and domain area distributions provide insight into the essential characteristics of growing and pinned lattices; however, they are not helpful for investigating different growing lattices.

Therefore, instead of focusing on the actual domain edge and domain area distributions, we avoid inadequate scaling state statistics by concentrating on the moments

of the distributions. We define the $m$th topological moment (i.e., the moment of the number of edges per domain),

$$\mu_m(T) \equiv \sum_{n=3}^{\infty} P(n)(n - \langle n \rangle)^m \quad (4)$$

and the $m$th domain area moment,

$$\mu_m(A) \equiv \int_0^{\infty} P(a/\langle a \rangle)(a/\langle a \rangle - 1)^m d(a/\langle a \rangle) \quad (5)$$

where $m$ is an integer with $1 \leq m \leq 4$.

In Fig. 3 we plot the moments of the late time topological distributions $\mu_m(T)$ for each lattice type. In particular, Fig. 3 shows the second through fourth moments of the topological distributions for domain growth simulations performed on the $s(1)$ lattice (at $T = \frac{2}{3}T_c$), the $t(1)$ lattice (an average of the $T=0$ and $T=\frac{1}{3}T_c$ data), the $s(1,2)$ lattice (at $T=0$) and the $t(1,2)$ lattice (at $T=0$). We determine each moment based upon data from 10 simulations at $t = 10^5$ MCS. (In order to improve statistics we often made use of the scaling state temporal invariance of the distributions by averaging the $10^5$ MCS data with data taken at $5 \times 10^4$ MCS.)

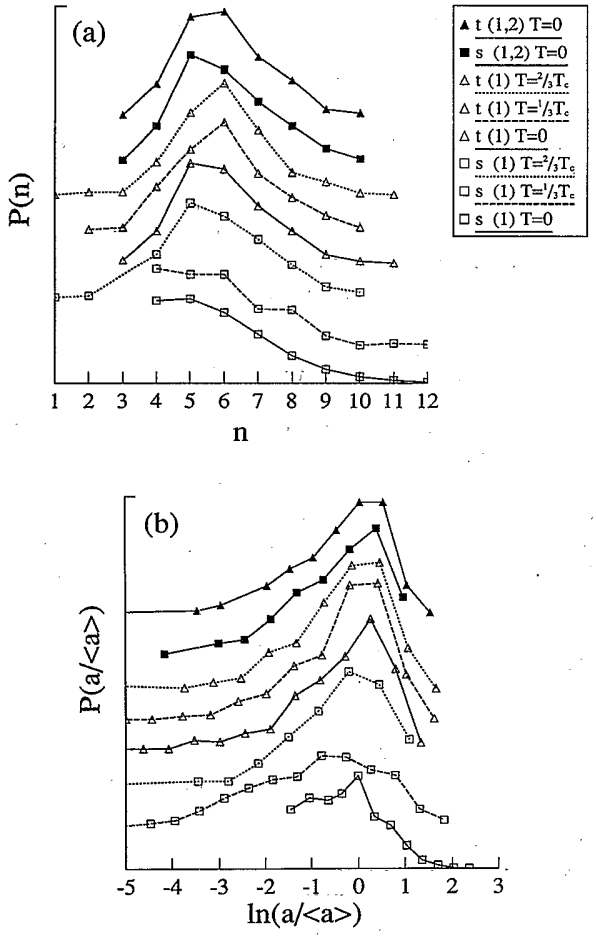


FIG. 2. Domain topology and area distributions for $s(1)$ and $t(1)$ at $T=0$, $\frac{1}{3}T_c$, and $\frac{2}{3}T_c$, and $s(1,2)$ and $t(1,2)$ at $T=0$. (a) Domain edge distributions. (b) Domain area distributions. Except for $s(1)$ at $T=0$, all data are taken in the scaling state; sample size is about 350 domains. Systems which grow normally [all except $s(1)$ at $T=0$ and $\frac{1}{3}T_c$] exhibit similar distributions.

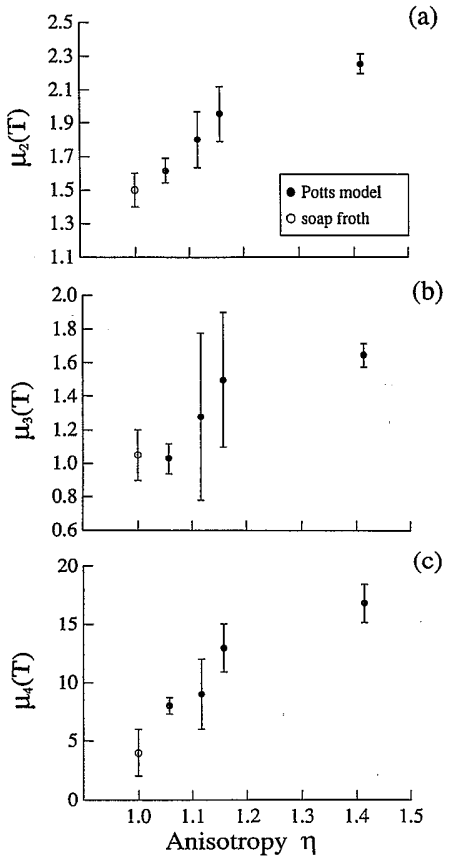


FIG. 3. Effect of lattice anisotropy on the moments of scaling state domain topology distributions. (a) $\mu_2(T)$. (b) $\mu_3(T)$. (c) $\mu_4(T)$. All moments decrease with decreasing anisotropy. Error bars indicate approximate range of fluctuations during the scaling state. Open circles denote the best experimental values for the two-dimensional soap froth.

All three moments increase monotonically with increasing anisotropy. For the sake of comparison with experimental data, we also show the moments for the topological distribution obtained from soap froth experiments. The soap froth results are in good overall agreement with the simulation data on the $t(1,2)$ lattice. This is not surprising since the anisotropy for soap froth should be identically unity (i.e., isotropic) and the $t(1,2)$ has the smallest anisotropy of any of the lattices investigated (i.e., about 1.06). The experimental topological moments obtained by Fradkov, Kravchenko, and Shvindlerman for two-dimensional grain growth in Al+$10^{-4}$ Mg foil at 460 °C are substantially larger than all corresponding scaling state Potts-model values, but are close to the values obtained for $s(1)$ at $T=\frac{1}{3}T_c$.[27] The large values of the moments may reflect an equilibration itransient, growth retardation due to the interaction of the grain boundaries with the surface, retardation due to impurity drag, or inherent anisotropy associated with the atomic lattice.

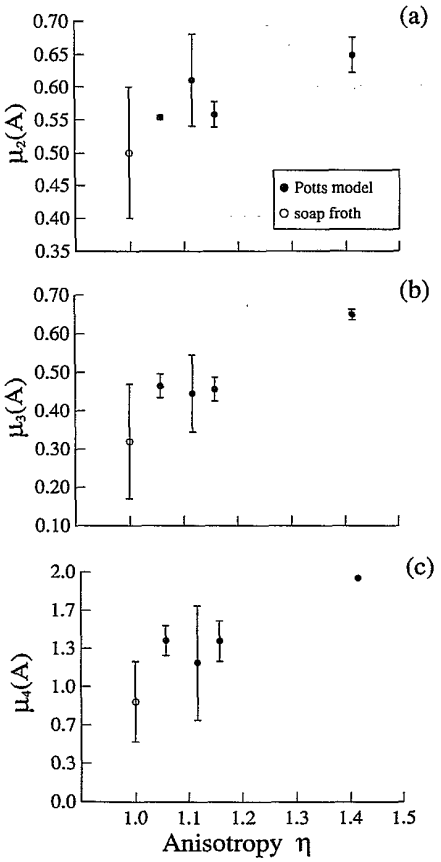


FIG. 4. Effect of lattice anisotropy on the moments of scaling state domain area distributions. (a) $\mu_2(A)$. (b) $\mu_3(A)$. (c) $\mu_4(A)$. All moments decrease with decreasing anisotropy. Error bars indicate approximate range of fluctuations during the scaling state. Open circles indicate best experimental values for the two-dimensional soap froth.

In Fig. 4 we plot the moments of the domain area distributions $\mu_m(A)$ as a function of lattice anisotropy for the same times and temperatures employed in Fig. 3. The moments tend to increase monotonically with the lattice anisotropy, although the scatter in the data is much more pronounced than for the topological moments.[9] Comparison with the soap froth data again shows that best agreement is obtained in the limit that the lattice anisotropy tends to one. Unfortunately, the moments of the Al thin film area distributions are not available.

## V. EFFECTS OF TEMPERATURE ON DISTRIBUTION

We plot the moments of the topological and domain area distributions as a function of temperature for $t(1)$ in Figs. 5(a) and 5(b), respectively. The topological and area moments are less strongly affected by changes in temperature than by changes in anisotropy (see Figs. 3 and 4), so that $\mu_2(T)$ and $\mu_2(A)$ are essentially independent of temperature. Nonetheless, $\mu_3(T)$ shows a small decrease with increasing temperature, while the error in $\mu_4(T)$ is too large to draw any conclusions. Similarly, $\mu_3(A)$ exhibits a slight decrease and $\mu_4(A)$ shows a strong decrease with increasing temperature. Overall, the topological and domain area distributions are affected similarly by changes in temperature.

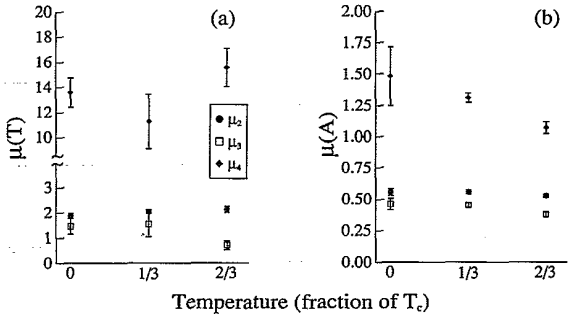


FIG. 5. Effect of temperature on the scaling state domain topology and size distributions for the $t(1)$ lattice. (a) Topological moments. (b) Area moments. Error bars approximate the range of fluctuations during the scaling state.

It is important to note that while the second moment of the domain area distribution changes by approximately 1% with temperature (over $0 \leq T/T_c \leq \frac{2}{3}$), it increases by about 15% when the lattice anisotropy is raised from 1 to 1.414. Similarly, the second moment of the topological distribution changes by 1% and 35%, respectively, as the temperature and anisotropy increase. Therefore lattice anisotropy is the more significant factor in determining the time invariant properties of the domain structure. As a consequence, it is imperative to select a lattice anisotropy and temperature for domain growth simulations that correspond to those of the experimental system.[9,11]

## VI. DISCUSSION AND CONCLUSIONS

von Neumann's law [Eq. (1)] implies that topological considerations dictate domain growth kinetics. Moreover, the local curvature of a domain wall controls its velocity. These two apparently unrelated features of domain growth are connected through the boundary condition that domain walls meet at angles which are determined by the domain wall energetics. The difference between the angles ($\theta_1$ and $\theta_2$) at which the domain wall meets a line drawn between its two end points defines the integral or total domain wall curvature ($K = \theta_1 - \theta_2$) and hence the net domain wall velocity ($v \propto K$—see Ref. 9). In an isotropic system, domain walls meet at 120°; hence a six-sided domain has zero net curvature and therefore neither grows nor shrinks. However, the discreteness of a lattice precludes a true, continuum vertex angle boundary condition. Therefore, in an anisotropic system, the orientational anisotropy may prevent domain walls which lie in preferred (low-energy) orientations from moving. In this case, domain vertices may stabilize at nonequilibrium angles, invalidating the fundamental assumptions of the von Neumann construction. Thus, when the lattice anisotropy is too large, the vertex boundary conditions are no longer strong enough to produce curvature in domain walls and domain growth stops. As the lattice anisotropy decreases below this threshold, there is an in-

creasing tendency to satisfy the energetic angular conditions at the vertices. In the limit that the anisotropy goes to unity, this tendency becomes infinitely strong, i.e., a boundary condition.

While lattice anisotropy changes the domain vertex characteristics, increasing temperatures do not affect the vertex constraints. Instead, thermal activation allows the domain walls to fluctuate out of the high symmetry directions associated with minima in the orientation dependence of the domain wall energy. Therefore thermal effects counteract the domain wall pinning tendency of the anisotropic lattice. This suggests that increasing temperature and decreasing lattice anisotropy both favor the satisfaction of the equilibrium vertex angular conditions and von Neumann's law, although by very different mechanisms.

Of all of the lattices examined in the present study, the $s(1)$ lattice has the highest anisotropy. At $T=0$, only a small degree of domain growth occurs before the domain walls become pinned. The $t(1)$ lattice has the next largest anisotropy, but it undergoes domain growth at all times. Therefore we conclude that the critical lattice anisotropy for domain growth in two dimensions $\eta_c$ lies between 1.157 and 1.414. We expect steady state domain growth to occur for all lattices with $\eta<\eta_c$ and to be precluded at $T=0$ for all lattices with $\eta>\eta_c$.

However, it is known that the $s(1,2)$ lattice with unequal first and second neighbor bond strengths pins domain growth at $T=0$, even though its Wulff plot anisotropy can be less than $\eta_c$, depending on the ratio of the bond strengths.[28] This observation suggests that the effective lattice anisotropy must be carefully defined for the pathological case of zero temperature. Because the energy of a $T=0$ system must monotonically decrease by the fastest path, in a lattice with nonuniform bond strengths, the more energetic bonds are preferred to the less energetic ones. Thus domain growth is governed and limited by growth on the sublattice of higher-energy neighbors. If that sublattice pins, the lower-energy sublattice will be insufficient to impart fluctuations to the domain walls, and domain growth will cease. Because the $s(1,2)$ lattice with unequal first and second neighbor bond strengths is composed of two interpenetrating $s(1)$ sublattices, it pins domain growth at $T=0$ with an effective anisotropy of $\eta_{\text{eff}}=\eta_{s(1)}>\eta_c$. Therefore the Wulff plot anisotropy $\eta$ of a lattice is equivalent to the effective system anisotropy at $T=0$ only for lattices with uniform bond strengths; in other lattices, the effective anisotropy is the Wulff plot anisotropy of the sublattice of the highest-energy bonds.

The initial stages of domain growth proceed faster with increasing temperature or decreasing anisotropy (see Fig. 1), in agreement with the above analysis of the effects of these variables on equilibrium vertex angles. Nonetheless, temperature plays only a minor role in domain growth provided $\eta<\eta_c$. That domain size is independent of temperature at late times (in the scaling regime) and that the domain size and topology distributions depend only weakly on temperature support this conclusion. For $\eta>\eta_c$, temperature plays the crucial role of effectively decreasing the lattice anisotropy.

The connection between domain topology and lattice anisotropy is due to the importance of the equilibrium vertex properties. Therefore we expect the width of the topological distributions to depend sensitively on the anisotropy. The presence of large widths of the grain topology distributions in thin metal films suggests that the anisotropy of the atomic lattice is large.[13] It is important to note, however, that this type of anisotropy is very different from that of the Potts model. In the Potts model, the anisotropy is due to the topology of an underlying lattice shared by all domains, while in the atomic case, each grain has a unique lattice orientation and the grain boundary energetics are sensitive to the atomic lattice orientations on both sides of the grain boundary. Additionally, the presence of impurities or solute atoms is known to impede boundary migration in metals.[29] As shown above for the Potts model, however, such slow growth is consistent with increased topological distribution width.

The excellent overall agreement (kinetics, topological distribution, domain size distributions) between the low lattice anisotropy Potts-model simulations and the soap froth suggest that the Potts model is a useful analog system for studying domain growth in a wide variety of physical systems. Additionally, the similarity between soap froth evolution, grain growth, and Potts-model domain growth demonstrate the universality of domain growth in highly degenerate systems and the general applicability of the von Neumann construction. A discrete lattice causes deviations from universal domain growth behavior by weakening the vertex angle boundary conditions which form the basis of von Neumann's law. The anisotropy inherent in discrete lattice simulations can be overcome by smoothing the Wulff plot of the lattice (e.g., by extending spin interactions to longer range) or by elevating the temperature at which the simulation is performed.

## ACKNOWLEDGMENTS

We are grateful to S. Ling and M. P. Anderson for providing their calculated values of the lattice anisotropies and to D. Rabson and R. Wolfe for helpful comments. E.A.H.'s work was supported in part by the National Science Foundation.

*Author to whom correspondence may be addressed.

[1]J. A. Glazier, M. P. Anderson, and G. S. Grest, Philos. Mag. B **62**, 615 (1990). J. A. Glazier, G. S. Grest, and M. P. Anderson, *Simulation and Theory of Evolving Microstructures,* edited by M. P. Anderson and A. D. Rollett (The Minerals, Metals and Materials Society, Warrendale, PA, 1990), p. 41.

[2]H. V. Atkinson, Acta Metall. **36**, 469 (1988).

[3]D. Weaire and N. Rivier, Contemp. Phys. **25**, 59 (1984).

[4]J. von Neumann, *Metal Interfaces* (American Society for Metals, Cleveland, 1952), p. 108.

[5]D. Weaire and J. P. Kermode, Philos. Mag. B **47**, L29 (1983); **48**, 245 (1983); **50**, 379 (1984).
[6]H. J. Frost and C. V. Thompson, *Computer Simulation of Microstructural Evolution,* edited by D. J. Srolovitz (The Metallurgical Society, Warrendale, PA, 1986), p. 33; H. J. Frost, C. V. Thompson, C L. Howe, and J. Whang, Scr. Metall. **22**, 65 (1988).
[7]K. Kawasaki, T. Nagai, and K. Nakashima, Philos. Mag. B **60**, 1399 (1989).
[8]A. Soares, A. C. Ferro, and M. A. Forres, Scr. Metall. **19**, 1491 (1985).
[9]J. A. Glazier, PhD. dissertation, University of Chicago, 1989 (unpublished).
[10]M. P. Anderson, G. S. Grest, and D. J. Srolovitz, Philos. Mag. B **59**, 293 (1989).
[11]M. P. Anderson, D. J. Srolovitz, G. S. Grest, and P. S. Sahni, Acta Metall. **32**, 783 (1984).
[12]G. S. Grest, D. J. Srolovitz, and M. P. Anderson, Acta Metall. **33**, 509 (1985).
[13]G. S. Grest, D. J. Srolovitz, and M. P. Anderson, Phys. Rev. B. **38**, 4752 (1988).
[14]D. J. Srolovitz, M. P. Anderson, G. S. Grest, and P. S. Sahni, Acta Metall. **32**, 1429 (1984).
[15]D. J. Srolovitz, M. P. Anderson, P. S. Sahni, and G. S. Grest, Acta Metall. **32**, 793 (1984).
[16]D. J. Srolovitz, G. S. Grest, and M. P. Anderson, Acta Metall. **33**, 2233 (1985).
[17]R. B. Potts, Proc. Cambridge Philos. Soc. **48**, 106 (1952).
[18]D. Kim and R. J. Joseph, J. Phys. C **7**, L167 (1974).
[19]S. Ling and M. P. Anderson (private communication).
[20]D. Weaire and Hou Lei (unpublished).
[21]J. A. Glazier and J. Stavans, Phys. Rev. A **40**, 7398 (1989).
[22]P. A. Beck, Adv. Phys. **3**, 245 (1954).
[23]J. A. Glazier, S. P. Gross, and J. Stavans, Phys. Rev. A **36**, 306 (1987).
[24]P. S. Sahni, D. J. Srolovitz, G. S. Grest, M. P. Anderson, and S. A. Safran, Phys. Rev. B **28**, 2705 (1983).
[25]Z. W. Lai, G. F. Mazenko, and O. T. Valls, Phys. Rev. B **37**, 9481 (1988).
[26]F. Haessner and S. Hofmann, *Recrystallization of Metallic Materials,* edited by F. Haessner (Riederer Verlag, Stuttgart, 1978), p. 76.
[27]V. E. Fradkov, A. S. Kravchenko, and L. S. Shvindlerman, Scr. Metall. **19**, 1291 (1985). The values are $\mu_2(T)=2.90\pm0.8$, $\mu_3(T)=5.01\pm3$, and $\mu_4(T)=44\pm20$.
[28]J. Viñals and M. Grant, Phys. Rev. B **36**, 7036 (1987).
[29]H. V. Atkinson, Acta Metall. **36**, 469 (1988).